



Charge stripe structure in Fe_{1+x}Te by STM

Yuki Kawashima^{a,*}, Koichi Ichimura^{a,b}, Junya Ishioka^a, Tohru Kurosawa^c, Migaku Oda^{c,b}, Kazuhiko Yamaya^a, Satoshi Tanda^{a,b}

^a Department of Applied Physics, Hokkaido University, Sapporo 060-8628, Japan

^b Center of Education and Research for Topological Science and Technology, Hokkaido University, Sapporo 060-8628, Japan

^c Department of Physics, Hokkaido University, Sapporo 060-0810, Japan



ARTICLE INFO

Article history:

Received 30 November 2012

Received in revised form

12 April 2013

Accepted 25 April 2013

by Xianhui Chen

Available online 23 May 2013

Keywords:

A. Iron-based superconductor

D. Charge stripe

E. STM

ABSTRACT

The electronic state of $\text{Fe}_{1.17}\text{Te}$ was investigated with atomic resolution by using STM. We discovered a charge stripe structure at 7.8 K for the first time. The wave vector of the charge stripe structure is along the a -axis or b -axis. Furthermore we found that the charge stripe occurred at the Fe layer. We also found a 9 meV gap structure on the Fermi surface by STS. The gap size is consistent with the mean field approximation with SDW transition temperature of 58 K.

© 2013 Elsevier Ltd. All rights reserved.

1. Introduction

How do we form a stripe structure using an isotropic interaction? An anisotropic interaction can create a stripe pattern by ordering in the same direction. There are many anisotropic interactive elements such as electric dipoles in ferroelectric materials, directors in liquid crystals and magnetic dipoles. When the anisotropic interaction is composed of an attractive direction and a repulsive direction, the elements that have the anisotropic interaction form a stripe structure. Can an isotropic interaction form a stripe pattern? Theoretically, isotropic particles can form a stripe pattern [1]. A coulomb interaction between charges is an isotropic interaction. The charge stripe structure was discovered in an organic conductor as charge ordering [2]. The electronic band structure of organic conductors is formed by anisotropic lattice structure. The charge order in an organic conductor is formed by electronic structural anisotropy. A cuprate superconductor also has a charge stripe structure [3,4]. The charge stripe structure had been predicted theoretically [5] as the pattern formed by carriers in Mott-insulator. The stripe structure on the cuprate superconductor was found as doped carrier with insulating antiferromagnetic domain [3]. Similar to cuprate superconductors, the charge stripe was found in other transition metal oxides such as nickelates [6], manganites [7,8] and cobaltates [9]. In these materials, holes form a stripe structure to minimize antiferromagnetic

domain wall. It is important that the stripe structure in Mott-insulator is stabilized only at commensurate doping. To study the isotropic interactive stripe structure, we need more simple charge stripe structure.

Recently, the iron-based superconductor was discovered [10,11]. Iron-based superconductors have different types of crystal structures including RFePnO (R =rare earth metals, $\text{Pn}=\text{P}, \text{As}$) [10,11], $(\text{Ba}, \text{K})\text{Fe}_2\text{As}_2$ [12], LiFeAs [13] and $\text{FeSe}_{1-\delta}$ [14]. The superconducting transition temperature of the iron-based superconductor is higher than 40 K for $\text{RFeAsO}_{1-x}\text{F}_x$ [15–17]. Therefore, the iron-based superconductor is called a new high T_c superconductor. The iron-based superconductor has a two-dimensional crystal structure and Fermi surfaces [18]. It is said that the hole Fermi surface at the Γ point and the electron Fermi surface at the M point induce a spin density wave (SDW) transition as a result of Fermi surface nesting [19,20]. It is noteworthy that direct evidences of SDW such as collective excitations have not been observed yet. The phase diagram of the iron-based superconductor reveals the coexistence of antiferromagnetism and superconductivity [11,21–23]. It is important that superconductivity is very close to magnetism in the iron-based superconductor [24]. The phase diagram of the iron-based superconductor is similar to that of an organic conductor and a cuprate superconductor. An organic conductor and a cuprate superconductor forms a charge order which usually competes with superconductivity. Then iron-based superconductors may form a charge ordering structure. FeX ($\text{X}=\text{S}, \text{Se}, \text{Te}$) family has the simplest composition and crystal structure among iron-based superconductors. It is easy to control the carrier concentration. Since FeX has no blocking layer, it is suitable to

* Corresponding author. Tel.: +81 11 706 7818.

E-mail address: yuki-k@eng.hokudai.ac.jp (Y. Kawashima).

study the electronic state of the conducting layer. In this letter, we report the charge stripe structure discovered in the iron-based superconductor by STM measurement.

2. Experimental

A single crystalline sample of Fe_{1+x}Te was grown by chemical vapor transport using iodine as the transport agent. Fe and Te were placed in an evacuated quartz tube with small amount of iodine. The quartz tube was heated at 700 °C for 1 week. The electronic properties of the sample were characterized by measuring the temperature dependence of resistivity and magnetic susceptibility. The DC resistivity was measured with the four probe method. The magnetic susceptibility was measured with a SQUID magnetometer while applying a magnetic field of 0.5 T. Temperature variable UHV-STM was used in the STM/STS study. Pr–Ir alloy wire was used as the scanning tip. To avoid absorption of gas, the sample was cleaved at 80 K in an ultra high vacuum. The crystal orientation was determined with an X-ray diffraction measurement, which shows that the crystal cleaves at the a – b plane.

3. Results and discussion

Temperature dependence of the resistivity and the magnetic susceptibility was measured to characterize the present sample. Fig. 1 shows temperature dependence of resistivity. The resistivity increases slightly from room temperature to 58 K with decreasing temperature. The resistivity exhibits a sharp peak at 58 K, and then it decreases from 58 K to 50 K. The resistivity increases slightly between 50 K and 0.5 K. The slope of the resistivity from room temperature to 58 K is larger than that from 50 K to 0.5 K. Fig. 2 shows temperature dependence of the magnetic susceptibility. The magnetic susceptibility obeys the Curie–Weiss law above 58 K and then rapidly decreases below 58 K. The temperature dependence shows a clear antiferromagnetic transition. The antiferromagnetic transition temperature is the same as the resistive peak temperature. By comparing temperature dependence of resistivity and antiferromagnetic transition temperature with the previous reports [25,26], the excess iron x is estimated as 0.17 for Fe_{1+x}Te . The composition was confirmed approximately by energy dispersive X-ray spectroscopy.

Fig. 3 shows an STM current image of the a – b surface taken at $T=7.8$ K with a bias voltage $V=700$ mV and a tunneling current $I=0.9$ nA. The crystal was cleaved at the a – b plane as mentioned above. The scanning area of the image is $10 \times 10 \text{ nm}^2$. Atoms are

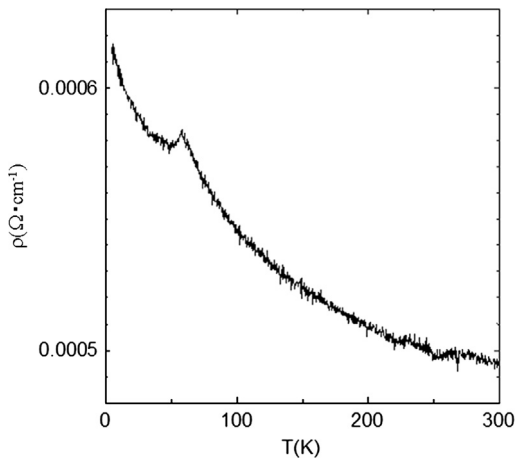


Fig. 1. Temperature dependence of resistivity of Fe_{1+x}Te ($x=0.17$).

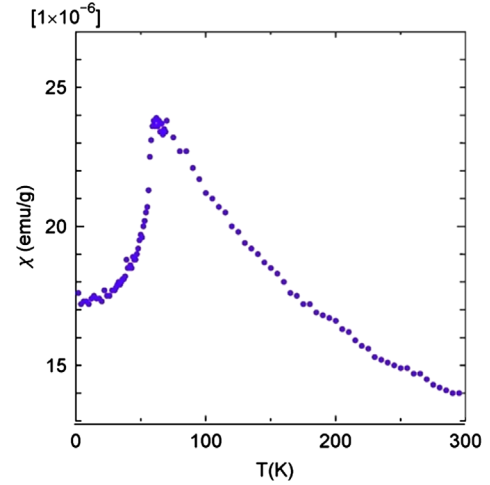


Fig. 2. (Color online) Temperature dependence of magnetic susceptibility of Fe_{1+x}Te ($x=0.17$).

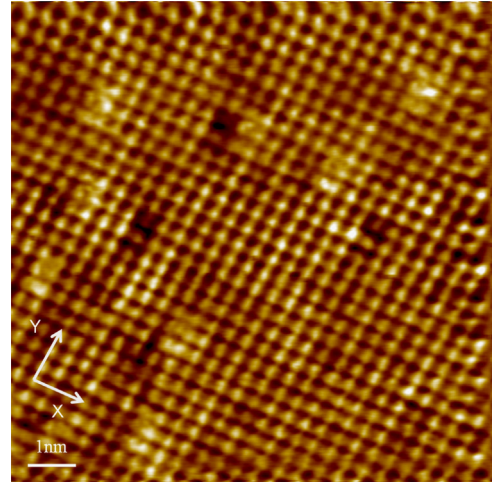


Fig. 3. (Color online) STM current image of Fe_{1+x}Te ($x=0.17$) at bias voltage $V=700$ mV and tunneling current $I=1.0$ nA. The image size is $10 \times 10 \text{ nm}^2$. The charge stripe wave vector is along the X arrow direction. Atoms connect and separate in the Y direction and X directions, respectively.

clearly resolved as bright spots, that form a square lattice with sides of 0.38 nm. The length of the lattice side corresponds to a Te lattice on an a – b layer. The bright spots in Fig. 3 are assigned as Te atoms. We found that the topmost layer was a Te layer that resulted from the cleaving. We discovered the stripe structure in the image. The atoms connect with each other along the Y arrow direction in Fig. 3. In contrast, no atoms connect with each other along the X arrow direction in Fig. 3. We first observed the charge stripe structure for the iron-based superconductor. The charge stripe wave vector direction is along the a -axis or b -axis. This charge stripe was observed at bias voltage in a range from 50 mV to 1000 mV.

To analyze the stripe structure in detail, we obtained a current image with a small scanning area. Fig. 4 shows a high-resolution current image obtained at 7.8 K. We took line profiles along lines A, B and C in Fig. 4. Fe atoms beneath a Te layer can be seen in this image. The image was taken at a bias voltage $V=700$ mV and a tunneling current $I=1.0$ nA. The image size is $3.3 \times 3.3 \text{ nm}^2$. In the image, there is a stripe structure of which wave vector is parallel to the lines A and B. The line profile A, which was taken along the blue line in the image, was obtained for both the direction of the stripe wave vector and on the Te atoms. There are other peaks indicated by blue arrows between the Te peaks in the line profile

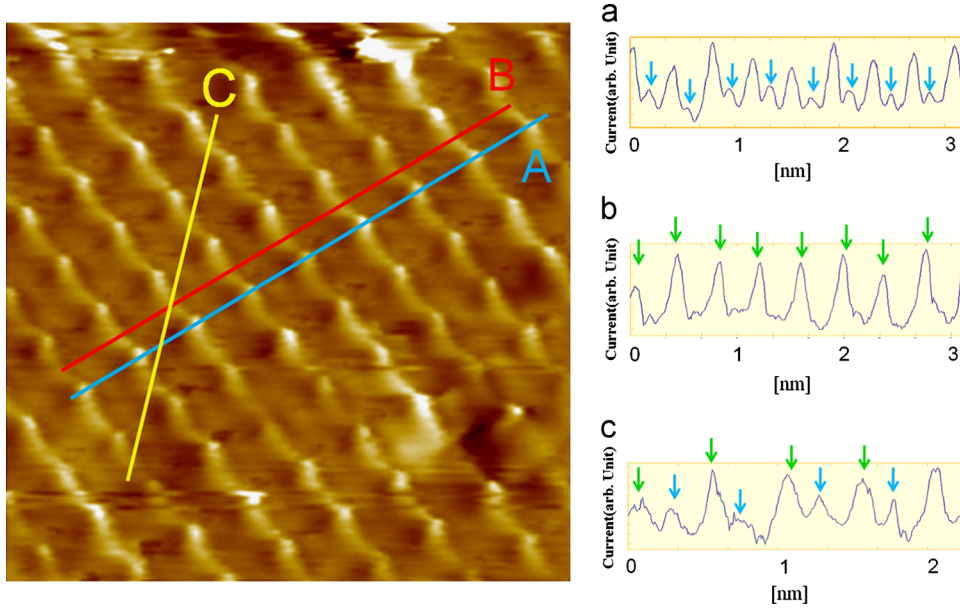


Fig. 4. (Color online) STM current image of Fe_{1+x}Te ($x=0.17$) at bias voltage $V=700$ mV and tunneling current $I=1.0$ nA. The image is 3.3 nm square. There are line profiles in the STM image. A, B and C in the STM image correspond to the line profiles signs. Peaks indicated by green and blue arrows correspond to the tunneling current from Fe atoms. The unlabeled peaks correspond to the tunneling current from Te atoms. The kind of atoms are decided by atomic distance.

A. It is likely that the top surface is Te layer as described above. The strong peaks correspond to the tunneling current from the Te atoms. The Fe layer is located 0.174 nm below the surface Te layer. We concluded that the weak peaks between the Te peaks were the tunneling current from the Fe layer beneath the Te layer. There are Fe atoms and Te atoms in the image. Line profile B is taken along the stripe structure between the Te atoms. There is a tunneling current only from the Fe layer in the line profile B. Line profile B shows that there is a tunneling current beneath the Fe layer. Fe atoms form a square lattice. The lattice side is 0.27 nm long. The lattice shape is rotated 45° in plane from the Te lattice. These Fe lattice details are consistent with the crystal structure. Line profile C is taken along the side of the Fe lattice. There are two types of tunneling current from the Fe atoms. This result shows that there are two types of Fe site. Each site has a different electronic state. The clear stripe structure is formed of two electronic states on the Fe layer. One is rich in charge and another is poor. We find that the stripe structure is caused by Fe atoms.

Fig. 5(a) shows the tunneling differential conductance on Fe_{1+x}Te ($x=0.17$) at 7.8 K and 80 K. At 80 K, the tunneling differential conductance curve is almost flat. At 7.8 K, the conductance curve has a gap structure at ± 9 mV indicated by black arrows in Fig. 5 (a). The tunneling spectra, where the differential conductance at $V=0$ is well reduced, show a gap structure at the Fermi level. Fig. 5 (b) shows d^2I/dV^2 curve which is a numerical differential of the differential conductance at 7.8 K. The kink positions indicated by black arrow were determined as first peak ($V > 0$) and dip ($V < 0$) in d^2I/dV^2 curve [27]. We assign the structure at ± 9 mV as the SDW gap. It is noteworthy that the shape of the differential conductance curve on the present material is similar to that of other iron-based superconductors such as the $\text{LaFeAsO}_{1-x}\text{F}_x$ [28] and $\text{SmFeAsO}_{1-x}\text{F}_x$ [29]. The existence of the pseudogap is suggested in these materials [28,29]. In Fig. 5, there are kink structure around ± 30 mV indicated by green arrows was determined as first dip ($V > 0$) and peak ($V < 0$) in d^2I/dV^2 curve. The kink structure at ± 30 mV is similar to the pseudogap structure observed in other iron-based superconductors [28,29].

The SDW transition temperature T_{SDW} of 58 K is determined by resistivity and magnetic anomalies. Correspondingly, the $2\Delta_{SDW}/kT_{SDW}$ is 3.60 which is almost consistent with the mean field value of 3.52.

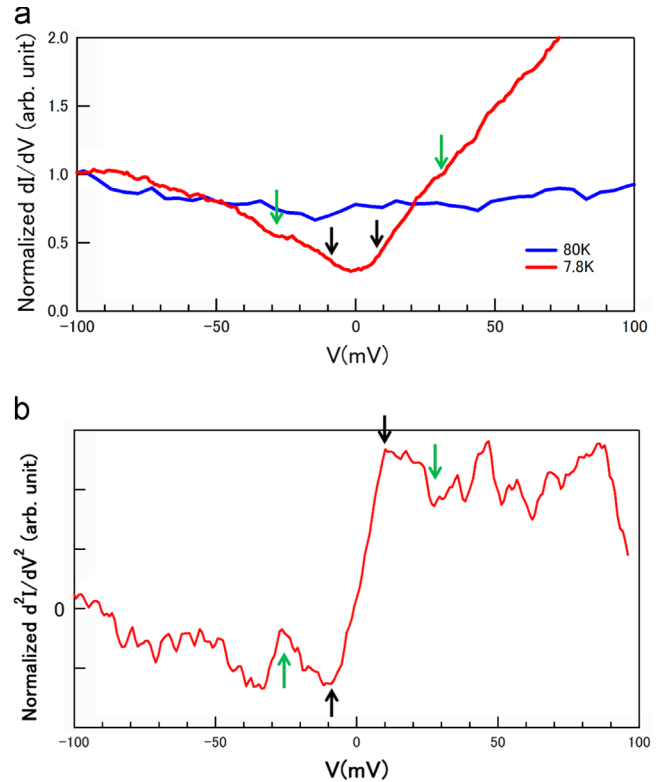


Fig. 5. (Color online) (a) Tunneling differential conductance on Fe_{1+x}Te ($x=0.17$) at 7.8 K and 80 K indicated by red and blue line, respectively. Black and green arrows indicate the SDW gap and the pseudogap, respectively. (b) Numerical differential of the differential conductance on Fe_{1+x}Te ($x=0.17$) at 7.8 K. Black arrows and green arrows correspond to the SDW gap and the pseudogap at the differential conductance curve.

The gap structure is caused by the SDW transition. We confirmed that the gap structure does not exist at 80 K. This gap structure is an indication of the SDW.

As a mechanism of the charge stripe in the present system, it might be a possible scenario in which the symmetry breaking of

the spin, charge and crystal structure occurs cooperatively [30]. In the model, SDW causes the charge stripe.

Organic conductors and cuprate superconductors have a strong coulomb interaction. Although they are called strong correlated electron systems, electrons in organic conductors have different characters from that in cuprate superconductors. Organic conductors are characterized by a small electron kinetic energy since the conduction is born by the overlap of molecular orbitals. The band width of organic conductors is about 0.5 eV [31]. Charge localization tends to occur when the electron kinetic energy is small. It is difficult to maintain itinerancy in a small kinetic energy. On the other hand, a cuprate superconductor is Mott-insulator based material which has strong onsite coulomb interaction. Strong onsite coulomb interaction makes charges localize with antiferromagnetic order. Carriers form stripe structure to minimize the antiferromagnetic domain wall at commensurate ratio of the doping. The driving force of the charge stripe in cuprate superconductors is the strong onsite coulomb interaction. An iron-based superconductor is based on metallic material which has several conduction bands. Therefore mechanism of forming stripe structure in iron-based superconductor is different from that in Mott-insulator materials. An iron-based superconductor has a large offsite coulomb interaction. This leads to coexistence of magnetism and superconductivity. We argue that the itinerancy and the offsite coulomb interaction play important role in forming charge stripe in iron-based superconductors. Moreover, we think that charge strip order can be formed in other iron-based superconductors as well as Fe_{1+x}Te with other iron concentration. The charge order structure and spin order structure in iron-based superconductors is similar to that of cuprate conductors. These order is important to study superconducting mechanism in the cuprate superconductor. Therefore, iron-based superconductors and cuprate superconductors have similar superconducting mechanism. We think that iron-based superconductor is a new type of low dimensional material, and it falls between a magnetic material and a superconducting material.

4. Conclusions

We discover the charge stripe structure on iron-based using STM/STS measurement. In $\text{Fe}_{1.17}\text{Te}$, the stripe structure is caused by the Fe atoms having different electronic states. With STS measurement, an SDW gap structure is observed at 7.8 K. We have a perspective that the charge stripe is occurred by the symmetry breaking as a result of SDW, and charge and spin order coexist.

Acknowledgment

The authors are grateful to Dr. K. Inagaki for valuable discussion. The authors also thank Professor S. Takayanagi for useful advices on resistivity measurements. This work was partially

supported by Grant-in-Aid for Scientific Research on Innovative Areas (No. 21110501) from Ministry of Education, Culture, Sports, Science and Technology of Japan.

References

- [1] G. Malescio, G. Pellicane, *Nat. Mater.* 2 (2003) 97.
- [2] T. Takahashi, Y. Nogami, K. Yakushi, *J. Phys. Soc. Jpn.* 75 (2006) 051008-1–051008-17.
- [3] J.M. Tranquada, B.J. Sternlieb, J.D. Axe, Y. Nakayama, S. Uchida, *Nature* 375 (1995) 561–563.
- [4] C. Howald, H. Eisaki, N. Kaneko, M. Greven, A. Kapitulnik, *Phys. Rev. B* 67 (2003) 014533-1–014533-9.
- [5] J. Zaanen, O. Gunnarsson, *Phys. Rev. B* 40 (1989) 7391–7394.
- [6] J.M. Tranquada, D.J. Buttrey, V. Sachan, J.E. Lorenzo, *Phys. Rev. Lett.* 73 (1994) 1003–1006.
- [7] C.H. Chen, S.-W. Cheong, H.Y. Hwang, *J. Appl. Phys.* 81 (1997) 4326–4330.
- [8] C. Renner, G. Aeppli, B.-G. Kim, Y.-A. Soh, S.-W. Cheong, *Nature* 416 (2002) 518–521.
- [9] A.T. Boothroyd, P. Babkevich, D. Prabhakaran, P.G. Freeman, *Nature* 471 (2011) 341–344.
- [10] Y. Kamihara, H. Hiramatsu, M. Hirano, R. Kawamura, H. Yanagi, T. Kamiyama, H. Hosono, *J. Am. Chem. Soc.* 128 (31) (2006) 10012–10013.
- [11] Y. Kamihara, T. Watanabe, M. Hirano, H. Hosono, *J. Am. Chem. Soc.* 130 (2008) 3296–3297.
- [12] M. Rotter, M. Tegel, D. Johrendt, *Phys. Rev. Lett.* 101 (2008) 107006-1–107006-4.
- [13] J.H. Tapp, Z. Tang, B. Lv, K. Sasmal, B. Lorenz, P.C.W. Chu, A.M. Guloy, *Phys. Rev. B* 78 (2008) 060505-1–060505-4.
- [14] F.-C. Hsu, J.-Y. Luo, K.-W. Yeh, T.-K. Chen, T.-W. Huang, P.M. Wu, Y.-C. Lee, Y.-L. Huang, Y.-Y. Chu, D.-C. Yan, M.-K. Wu, *Proc. Natl. Acad. Sci. U.S.A.* 105 (2011) 14262–14264.
- [15] M.H. Chen, T. Wu, G. We, R.H. Liu, H. Chen, D.F. Fang, *Nature* 453 (2008) 761–762.
- [16] Z.-A. Ren, J. Yang, W. Lu, W. Yi, X.-L. Shen, Z.-C. Li, G.-C. Che, X.-L. Dong, F. Zhou, Z.-X. Zhao, *Europhys. Lett.* 82 (2008) 57002-1–57002-2.
- [17] E.P. Khlybov, O.E. Omelyanovsky, A. Zaleski, A.V. Sadakov, D.R. Gizatulina, L. F. Kulikova, I.E. Kostuleva, V.M. Pudalov, *J. Exp. Theor. Phys.* 90 (2009) 387–390.
- [18] M. Rotter, M. Tegel, D. Johrendt, I. Schellenberg, W. Hermes, R. Pottgen, *Phys. Rev. B* 78 (2008) 020503-1–020503-4.
- [19] A. Subedi, L. Zhang, D.J. Singh, M.H. Du, *Phys. Rev. B* 78 (13) (2008) 134514.
- [20] Y. Xia, D. Qian, L. Wray, D. Hsieh, G.F. Chen, J.L. Luo, N.L. Wang, M.Z. Hasan, *Phys. Rev. Lett.* 103 (2009) 037002-1.
- [21] H. Chen, Y. Ren, Y. Qiu, W. Bao, R.H. Liu, G. Wu, T. Wu, Y.L. Xie, X.F. Wang, Q. Huang, X.H. Chen, *Europhys. Lett.* 85 (2009) 17006-1–17006-5.
- [22] F.X. Wang, T. Wu, G. Wu, H.R. Liu, H. Chen, L.Y. Xie, H.X. Chen, *New J. Phys.* 11 (2009) 45003.
- [23] Y. Mizuguchi, Y. Takano, *J. Phys. Soc. Jpn.* 79 (2010) 102001-1–102001-18.
- [24] C. de la Cruz, Q. Huang, J.W. Lynn, J. Li, W. Ratcliff, J.L. Zaresty, H.A. Mook, G. F. Chen, J.L. Luo, N.L. Wang, P. Dai, *Nature* 453 (2008) 899–902.
- [25] M.H. Fang, H.M. Pham, B. Qian, T.J. Liu, E.K. Vehstedt, Y. Liu, L. Spinu, Z.Q. Mao, *Phys. Rev. B* 78 (2008) 224503.
- [26] T.J. Liu, X. Ke, B. Qian, J. Hu, D. Fobes, E.K. Vehstedt, H. Pham, J.H. Yang, M. H. Fang, L. Spinu, P. Schiffer, Y. Liu, Z.Q. Mao, *Phys. Rev. B* 80 (2009) 174509.
- [27] Y. Kawashimaa, K. Ichimuraa, J. Ishioka, T. Kurosawa, M. Oda, K. Yamaya, S. Tanda, *Phys. B: Condens. Matter* 407 (2012) 1796–1798.
- [28] K. Ichimura, J. Ishioka, T. Kurosawa, K. Inagaki, M. Oda, S. Tanda, H. Takahashi, H. Okada, Y. Kamihara, M. Hirano, H. Hosono, *J. Phys. Soc. Jpn.* 77 (Suppl.) (2008) 151–152.
- [29] Y. Kawashima, K. Ichimura, T. Kurosawa, M. Oda, S. Tanda, H. Takahashi, H. Okada, Y. Kamihara, H. Hosono, *Physica C* 470 (2010) S315–S316.
- [30] To be discussed elsewhere.
- [31] T. Ishiguro, K. Yamaji, G. Saito, *Organic Superconductors*, 2nd Edition, Springer, Berlin, 1997.